Chapter 2

REFINEMENTS OF THE IMPEDANCE-BASED STRUCTURAL HEALTH MONITORING TECHNIQUE

Part I. Compensating Effects of Temperature Changes

2.1 Introduction

In almost all practical field applications, the structure that is being monitored is constantly undergoing changes due to external boundary and environmental conditions. This change, in most cases, is considered to be normal and a part of the everyday use of the structure. Examples of the factors that lead to this change are loading of the structure, vibration of the structure and change in the ambient temperature. These factors not only effect the structure but also the equipment that is used to monitor its integrity. For example, temperature changes not only affect the structure in question, but also the piezoelectric sensors mounted on the structure. The effects of these factors on the impedance signature and the capability of the technique to distinguish and determine damage, are the motivation of this research and main issues that must be dealt with before full-scale development and commercialization can take place.

In this chapter, the temperature variation of PZT sensors and the structures was investigated and the compensation technique for this variation was established to extend damage detection capability of the impedance-based health monitoring technique. Three proof-of-concept experiments, including a bolted pipe joint, a composite reinforced aluminum plate and a precision part (gear), were conducted to verify the effectiveness of the compensation technique under significant temperature variations.

2.2 Temperature effects on Piezoelectric Materials

Piezoelectric materials have been known to have strong temperature dependency regarding their basic properties. Among the temperature dependent property constants of piezoelectric materials, the dielectric constant, ε_{33}^{T}, exhibits most significant effect on electrical impedance (Piezo systems, 1998). It modifies the first term of equation (1.3), the capacitive admittance, causing a baseline shift of the electrical impedance. The piezoelectric coupling constant and complex Young's modulus also result in baseline shift, but the effect on the overall impedance can be negligible compared with dielectric constant.

Previous experimental work (Krishnamurthy *et al*., 1996) of the effects of temperature on a free PZT PSI-5A shows that an increase in temperature leads to a decrease in the impedance magnitude. Even though the piezoceramic PSI-5A has been shown to have a nonlinear relation of its dielectric constant and piezoelectric factor with temperature, the temperature range of 25 to 75 $^{\circ}C$ is small enough to consider only the region linear. This work also showed that if the variation of impedance with temperature is normalized to eliminate the effect of impedance magnitude changes, then the impedance variation becomes independent of frequency.

Experiments in the laboratory on various case studies have shown that the real part of the electrical impedance is more reactive to damage or change in the structure integrity than the magnitude or imaginary part of the electrical impedance. The change in the impedance signature of the PZT-structure combination is solely due to the contribution of the changing impedance of the structure. This sensitivity characteristic is exhibited in the resistive portion of the impedance signature (real part). The reactive portion (imaginary part) of the impedance remains unchanged (or changes a little), any change in this portion is more likely due to changes in boundary conditions such as loading effects, temperature changes and increase in test wire length. Figure 2.1 shows the change of the real part of electrical impedance of free PZT PSI 5A versus change in temperature. Instead of a downward shifting

of impedance curve as in the case of electrical impedance magnitude (Krishnamurthy *et al*., 1996), the resistive portion of the electrical impedance shows a relatively insignificant change, keeping the magnitude unchanged or changed a little. This result suggests that the impedance-based health monitoring method must utilize the resistive portion of the electrical impedance for the response change due to the presence of damage to minimize the effects of the temperature on the piezoelectric material itself.

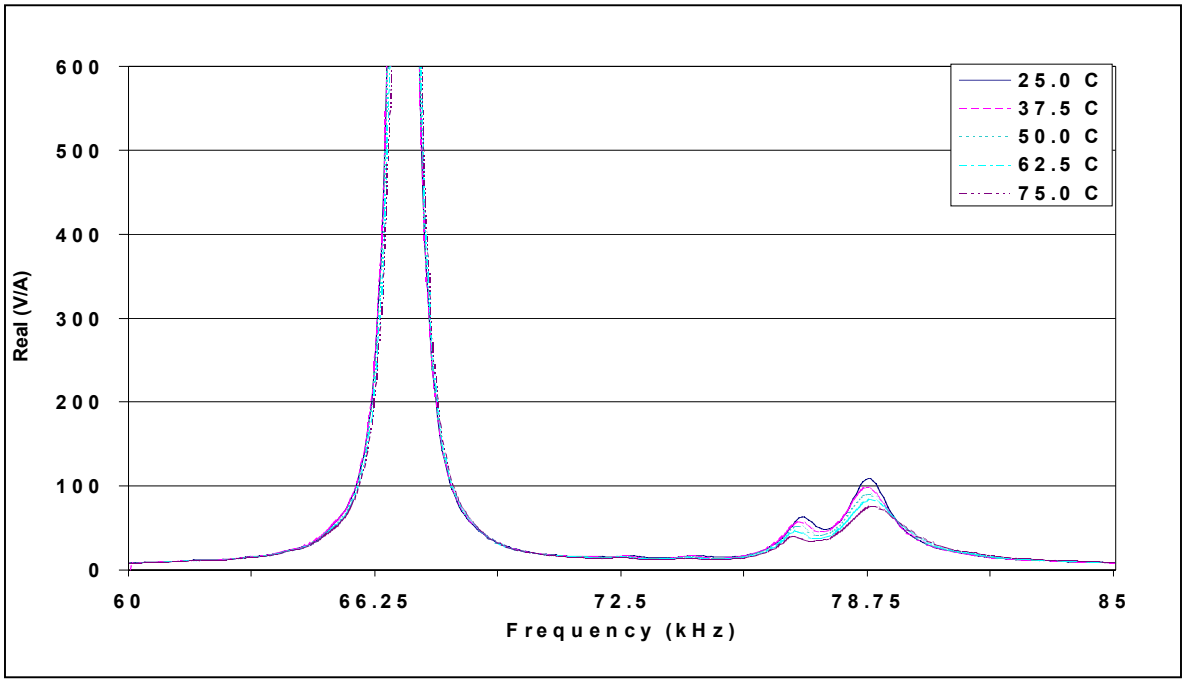

Figure 2.1 For a free PZT PSI-5A, an increase in temperature leads to a small magnitude change in the real part of electrical impedance.

2.3 Temperature Effects on the Monitored Structures

The Young's modulus of the host material varies slightly with temperature and the thermal expansion of the material will induce stresses in constrained structures. Woon and Mitchel (1996a, 1996b) have shown experimentally and analytically that temperature has a distinct effect on the dynamic properties of structures, which is dependent on boundary conditions, temperature distribution and structures' material. However, precise and detailed material property data for slight temperature variation is lacking. Most previous work is concerned with very large magnitudes of temperature variations at extremely high temperatures, as usually encountered in the aerospace field. In addition, in complex structures, developing an analytical model of the temperature effects would be a tremendous task. For this reason, a simple model (1-D beam) and empirical approach was used to study the effect of temperature on the host structure.

A simple steel beam with free-free boundary condition is used for the analytical study of the variations in structural response caused by temperature changes. Only the shifts in resonant frequencies are discussed here. Experimental investigations have shown that the Young's modulus of carbon steel varies linearly with temperature (Cook *et al*., 1990). Thus, the Young's modulus can be written as functions of temperature based on its rates of change around reference temperature,

$$E(T) = E_0 + \frac{\partial E}{\partial T}(T - T_0) = E_0 + \beta \Delta T \tag{2.1}$$

where E is the Young's modulus at the measuring temperature, E_0 is the Young's modulus at the reference temperature, T is the measuring temperature, T_0 is the reference temperature, and β is the linear change in Young's modulus with respect to temperature. β is negative as shown in Woon and Mitchel (1996b).

It is also shown experimentally that the coefficient of linear thermal expansion of steel is approximately constant over the small temperature range. Therefore, the structural dimensions can be written as functions of temperature,

$$w = w_0(1 + \alpha\Delta T) \tag{2.2a}$$

$$l = l_0(1 + \alpha\Delta T) \tag{2.2b}$$

$$t = t_0(1 + \alpha\Delta T) \tag{2.2c}$$

where w is the width of the beam, w_0 is the reference width of the beam, l is the length of the beam, l_0 is the reference length of the beam, t is the thickness of the beam, t_0 is the reference thickness of the beam, and α is the mean coefficient of linear thermal expansion.

Due to the thermal expansion, the beam density per unit volume also varies with temperature. Since the mass of the beam remains the same regardless of temperature and the beam is assumed isotropic, we can write

$$\rho = \frac{M}{V} = \frac{M}{w_0 l_0 t_0 (1 + \alpha\Delta T)^3} = \frac{M}{V_0 (1 + \alpha\Delta T)^3} = \frac{\rho_0}{(1 + \alpha\Delta T)^3} \tag{2.3}$$

where M is the mass of the beam, ρ is the mass density of the beam, ρ_0 is the mass density of the beam at the reference temperature, V is the volume of the beam, and V_0 is the volume of the beam at the reference temperature.

The natural frequencies of the free-free beam in bending has well-known solutions for the first several modes (Inman, 1994), which is:

$$f_r = \frac{\beta_r^{\,2}}{2\pi}\sqrt{\frac{EI}{\rho A}} \tag{2.4}$$

where f_r is the natural frequency in Hz of the r[th] bending mode, β_r is the weight function for the r[th] bending mode, I is the area moment of inertia of the beam, and A is the area of the cross section of the beam.

For a beam with a constant rectangular cross section, $I = wt^3/12$ and $A = wt$. Then, Equation (2.4) can be rewritten to account for the temperature dependency of the material properties by incorporating Equations (2.1) - (2.3) as follows:

$$f_r = \frac{(\beta_r l)^2 t_0}{4\pi l_0^{\,2}} \sqrt{\frac{(E_0 + \beta\Delta T)(1+\alpha\Delta T)}{3\rho_0}} \tag{2.5}$$

and, since the natural frequency at the reference temperature can be expressed as,

$$f_{r0} = \frac{(\beta_r l)^2 t_0}{4\pi l_0^{\,2}} \sqrt{\frac{E_0}{3\rho_0}} \tag{2.6}$$

Then, the ratio of the natural frequency shifting to the reference frequency with temperature can be defined as follows:

$$\frac{f_r}{f_{r0}} = \sqrt{\frac{(E_0 + \beta\Delta T)(1+\alpha\Delta T)}{E_0}} \tag{2.7}$$

Considering the material properties of steel, (E_0 = 2.1 x 10^{11} N/m^2, α = 6.0 x 10^{-6}, β = -3.7 x 10^7 N/m^2), the term $(E_0 + \beta\Delta T)$ in this equation is dominant for changes in temperature. Figure 2.2 shows the ratio of the natural frequency of steel beam to the natural frequency at the reference temperature, f_r/f_{r0}, as a function of temperature. The reference temperature is 75 ºF. The result indicates that an increase in temperature leads to a decrease in resonant frequencies. This is due to the Young's modulus effect, because β is a negative value. On the other hand, the thermal expansion increases the resonant frequencies of beam, however

the effect is very small. This result suggests that increase in temperature leads to shifting resonant frequencies, shifting the sharp peaks horizontally in impedance versus frequency plot.

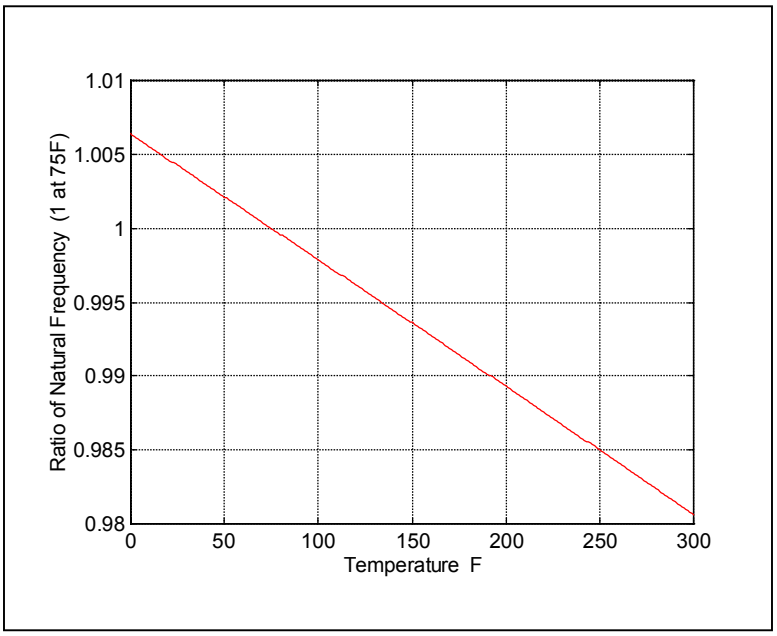

Figure 2.2 Predicted ratio of natural frequency of the steel beam shifting with temperature (reference temperature = 75 ºF)

Experiments were performed to investigate the effects of temperature on the peak frequency and magnitude of the electrical impedance of the beam. First, measurements were made at low frequency range to compare with the results of conventional modal analysis, and then the same experiment was conducted at high frequency range, 70-80 kHz, at which the impedance-based technique is normally used.

The experiments were carried out on a single carbon-steel beam (30 mm x 250 mm x 0.85 mm) with PZT sensor-actuator bonded in the middle. Figure 2.3 is a schematic of the experimental setup. The beam was suspending inside an oven equipped with a temperature controller. Using this controller, the temperature in the oven was varied from 25 $^{\circ}C$ to 75 $^{\circ}C$

in steps of 12.5 $^{\circ}C$. For the first experiment, the beam was excited using an PSI-5A piezoceramic bonded in the middle. The measurements were taken over the 0-5kHz frequency range. A KISTLER miniature accelerometer, model 8728A500 (temperature coefficient of sensitivity : –0.03 %/$^{\circ}F$), was used to measure the frequency response function (FRF) of this structure. Simultaneously, an HP4194 electrical impedance analyzer was used for the measurement of the PZT's electrical impedance. These measurements were taken over the same frequency range at 1.25 Hz interval. The electrical impedance was then measured again over the high frequency range (70–80 kHz). Each meaurement was taken after steady-state temperatures had been reached.

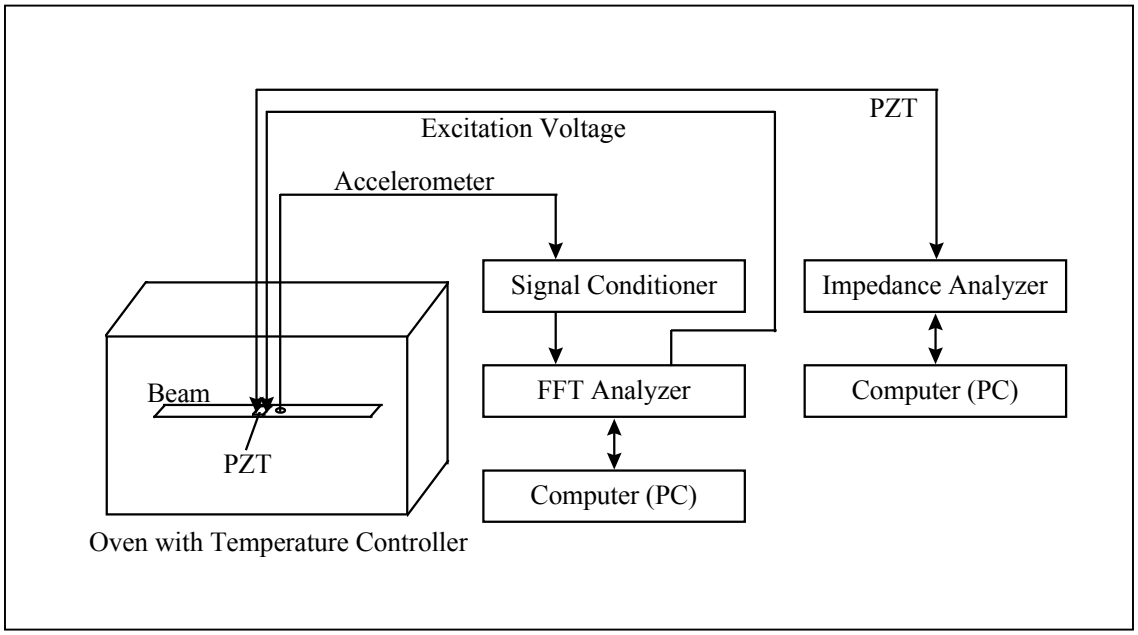

Figure 2.3 Schematic of the experiment on temperature effects

The FRF measurements of the free carbon-steel beam are shown in Fig. 2.4. Only 3-5 kHz frequency range is shown. It is observed that an increase in temperature leads to shifting of resonant frequencies and fluctuations in peak response magnitude. The shifting of the peak frequencies indicates a variation in the structural stiffness, caused by changes in the material and structural dimensional properties. Likewise, variations in the peak response magnitude suggest a damping-related phenomenon. Hence, it can be said that a combination of both structural stiffness and damping variations are involved in temperature change. Incidentally, the resonance near 3.6 kHz is the 10^{th} bending mode and 4.4 kHz is the 11^{th} bending mode

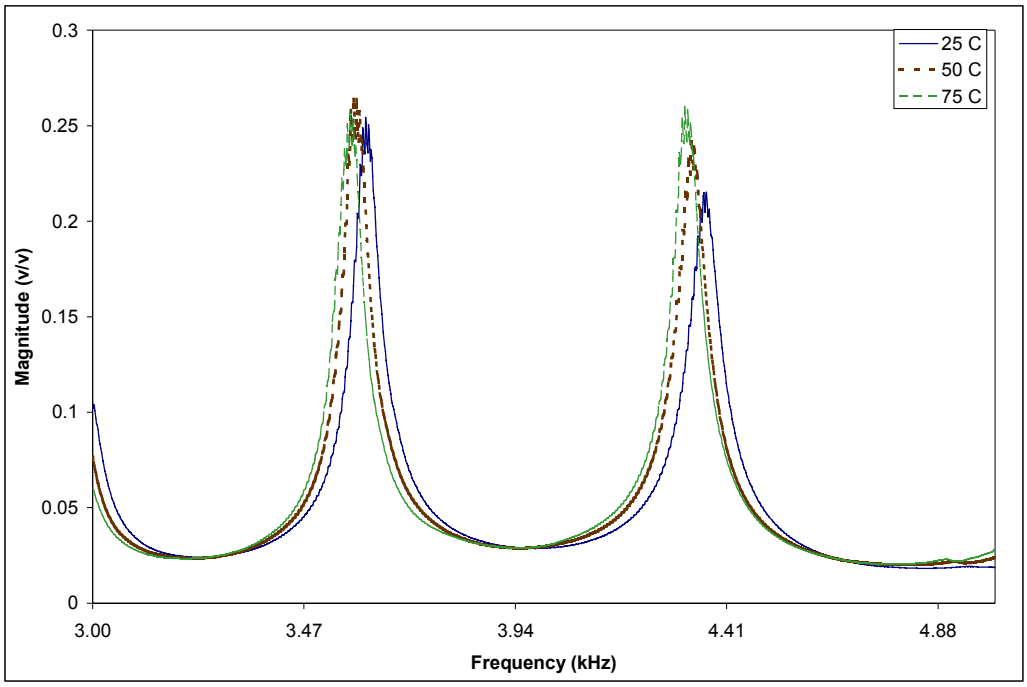

Figure 2.4 FRF measurement of the carbon-steel beam with the temperature change

The impedance versus frequency plot results indicate that the change in temperature leads to a horizontal shift and magnitude change of the impedance peak, as shown in Fig. 2.5. A real part, an imaginary part and a magnitude are shown in figure. All these plots indicate that the change in temperature leads to a horizontal shift, and the peak frequencies of these plots match with those of the FRF plot. In the imaginary part and the magnitude plots, a drift,

which is caused by the capacitive property of PZT, can be found. The horizontal shifts of resonant frequencies from the experiment ranges from 0.994 to 0.999 for first 20 modes, while the analytically predicted value is 0.998 for a change of 12.5 $^{\circ}C$. The error between the predicted and measured natural frequencies is less than 1%. Note that the peak frequencies of both plots are matching, verifying that the electrical impedance of piezoceramic materials constitute a unique signature of the dynamic behavior of the structure. Figure 2.6 is presenting the impedance versus frequency plot with change in temperature at high frequency range. As expected, and compared with low frequency ranges, the horizontal shifts of impedance peaks are significant. Changes in the peak level also can be found.

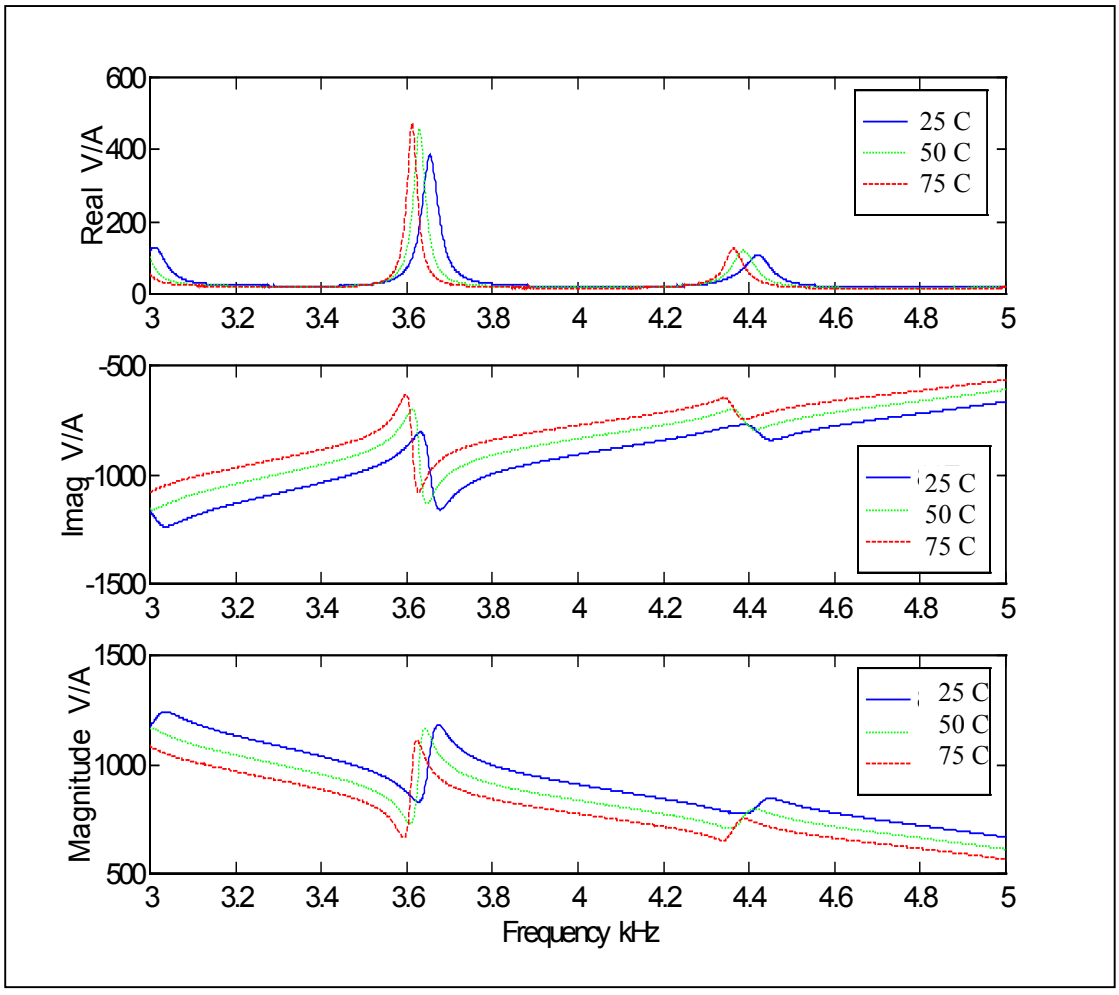

Figure 2.5 Real part of electrical admittance of the carbon-steel beam with the temperature change.

In summary, with increasing temperature, resonant frequency is found decrease and the magnitude of electrical impedance (real part) is also expected to decrease. Therefore, these small temperature variations could have a significant impact on the impedance based NDE technique, modifying the electrical impedance especially at high frequency range where we have found most useful for this NDE technique (in excess of 30 kHz).

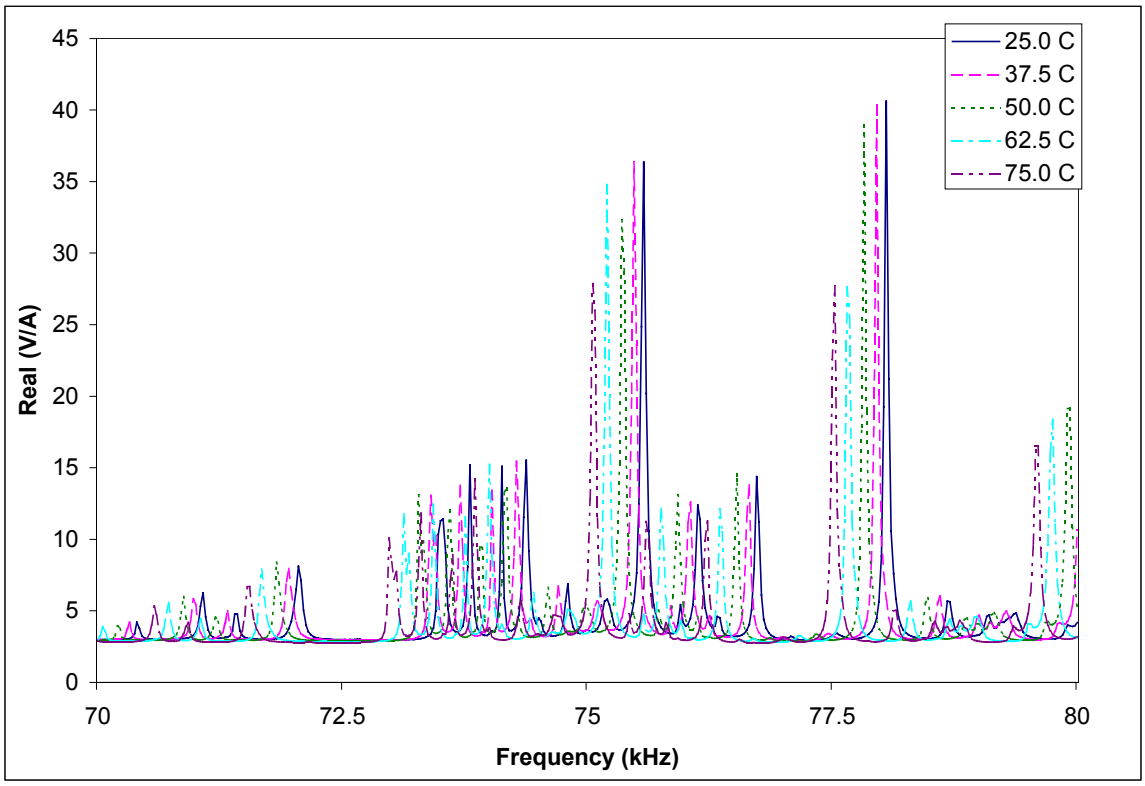

Figure 2.6 Real part of electrical impedance of the carbon-steel beam with the temperature change at high frequency range.

2.4 The Compensation Procedure

As seen in the previous sections, the change in temperature results in important changes in the dynamic response of both PZT sensor and the structures. The impedance variation associated with temperature change could lead to the wrong conclusion regarding the integrity of the structure in question. Therefore, a software correction technique in the impedance-based health monitoring technique is developed to minimize the effects of the ambient or structural temperature changes. This variation should be taken into account when planning and designing the health monitoring system, in order to avoid false alarms.

Two temperature compensation techniques were previously proposed at CIMSS, however, the method presented by Sun *et al.* (1995), which uses cross correlation to correct the horizontal shift in the signature pattern, does not work if the signature has even a small distortion. The method presented by Krishnamurthy *et al*. (1996) requires preliminary impedance measurements of free PZTs and does not consider the temperature effects on the structure being monitored.

The temperature compensation technique should account for the temperature effect on the structure being monitored, as well as the PZT sensors. In complex structures, however, a compensation technique based on the analytical modeling of the temperature effects may not be practical due to the complex constitutive thermal-electrical-mechanical models of piezoelectric material and due to the requirement of the complicated modeling of the structure. For this reason, an empirical approach was used to minimize the effect of temperature on the impedance-based technique.

Based on the observation from the previous experiment, the vertical and horizontal shifts of impedance pattern due to the temperature change can be considered as uniform in a narrow frequency range that is, the entire signature pattern essentially translates vertically and horizontally. On the other hand, the impedance variation due to structural damage is

somewhat irregular. This feature allows removing the temperature effect from the impedance-based technique.

The procedure to apply the correction scheme is based on the reconstruction of the damage metric. At first, the vertical shift is simply corrected by the difference in overall average value of the original and the interrogated impedance patterns as shown below:

$$\delta_v = \frac{\sum_{i=1}^{n} \mathrm{Re}(Y_{i,2})}{n} - \frac{\sum_{i=1}^{n} \mathrm{Re}(Y_{i,1})}{n} \tag{2.8}$$

where δ_v is the vertical shift, $Y_{i,1}$ is the original impedance at frequency interval i (baseline measurement), $Y_{i,2}$ interrogated impedance at frequency interval i (subsequent measurement), and n is the number of data points measured.

Next, the data are interpolated to increase the frequency resolution if necessary. The number of data points or frequency lines, n, increases to N. Finally, the horizontal shift is searched by the iteration to minimize the damage metric, which is defined as follows:

$$M = \sum_{i=1}^{N} \left[\mathrm{Re}(Y_{i,1}) - \left\{ \mathrm{Re}(Y_{i+\delta_h,2}) - \delta_v \right\} \right]^2 \tag{2.9}$$

where M is the damage metric and δ_h is the horizontal shift (data point shift). The value of δ_h can be found under a preset criteria (for example, ±10 or ±20), searching for the minimum value of damage metric. Thus, optimal sets of values of δ_v and δ_h, minimizing the effect of the temperature variation can be obtained.

The result of the temperature compensation of the previous beam experiment is shown in Fig. 2.7. The solid $25\,^{\circ}C$ line is the reference impedance measurement against which the temperature contaminated impedance will be compensated. As can be seen, it is difficult to distinguish from the reference solid line, compared with Fig. 2.6. The damage metric is small enough to indicate no damage is present. However, it should be noted that, in complex structures, there would be more factors to be considered, such as thermal-induced stress, boundary condition effects and temperature distribution which are not present in this test case. Hence, the temperature variation in complex structures is expected to be more complicated than illustrated in this test.

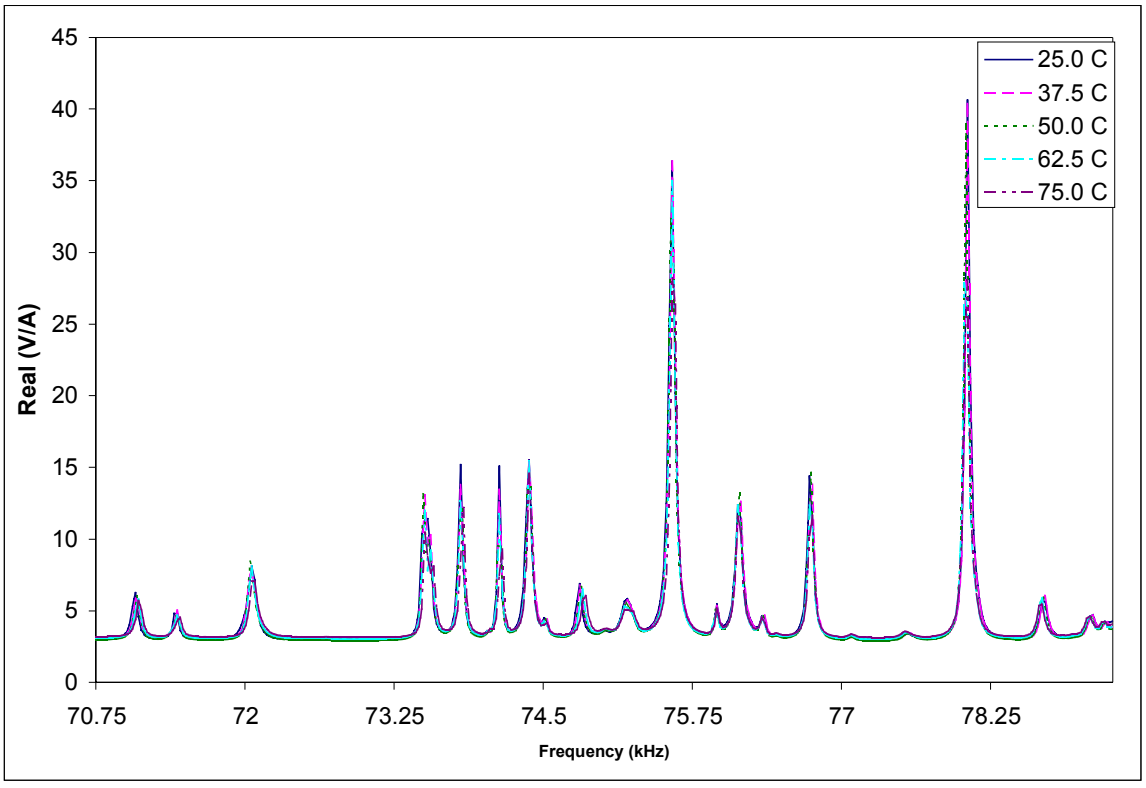

Figure 2.7 Compensated electrical impedance of the carbon-steel beam with the temperature change.

2.5 Proof-of-Concept Applications

To date, the impedance-based health monitoring technique has been applied to several complex structures. However, most of applications are constrained under the strict boundary and environmental conditions to minimize the effects of unknown variations, especially temperature variations. With the temperature compensation technique, the experimental investigation was made under the varying temperature conditions for the first time, including the detection of a loose connection, abrasive wear in gears, and delamination in composite structures (Park *et al*. 1999).

2.5.1 A Bolted Pipe Joint

A bolted flange-pipe joint is used in the experimental setup, as can be seen in Fig. 2.8. This model was chosen because this is complex enough to validate the temperature compensation technique, and temperature variations in pipeline systems are quite significant in application. The model consists of two 50 mm diameter, 150 mm long steel pipes and two flanges jointed by four d12 mm bolts. A PZT (Piezo Systems PSI-5A, 12.7 mm x 12.7 mm x 0.254 mm) was bonded on the flange for the acquisitions of impedance over the selected frequency range (70-80 kHz) at five temperature levels; 25, 37.5, 50, 62.5 and 75 $^{\circ}C$. After measuring the impedance at each level of temperature, damage is simulated in the joint by loosening one bolt (1/6 turn) located across the PZT sensor, at temperature 50 $^{\circ}C$. This damage, which still can be considered in the incipient stage, does not alter the integrity of the pipe joint. All of the impedance measurement were compensated and compared against the reference measurement, taken at temperature 25 $^{\circ}C$.

The results are shown in Fig. 2.9, for visual comparison. As expected, relatively large impedance variations were observed, compared with the 1-D beam case, as can be seen in the figure. The fluctuations of magnitude are clearly observed as well as the horizontal shift of resonant frequencies. The exact reason for this large change could not be exactly explained, but it is believed that damping-related phenomena caused by bolted joints would be a dominant factor in this variation. Figure 2.10 shows the compensated impedance

measurements at each step of temperature and damage. The compensated impedance curves do not exactly match the reference impedance. One, however, can clearly observe the difference between the temperature variation and the damage by this compensation technique, while it is difficult to distinguish between uncompensated impedance measurements. As can be seen from damage metric chart in Figure 2.10, temperature variation could lead to wrong conclusion regarding the integrity of the structure, not accurately predict the presence of real damage. However, the compensation technique minimizes the temperature variation to a great extent and is able to provide a definite signal to indicate the presence of damage.

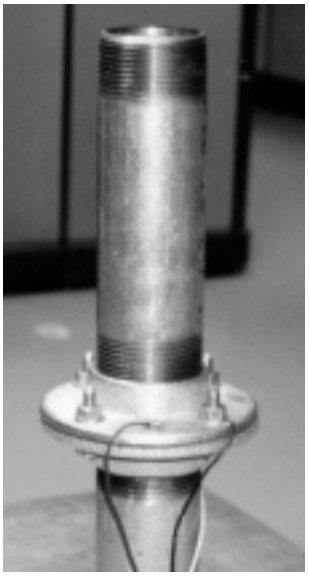

Figure 2.8 Experimental setup of bolted pipe joint

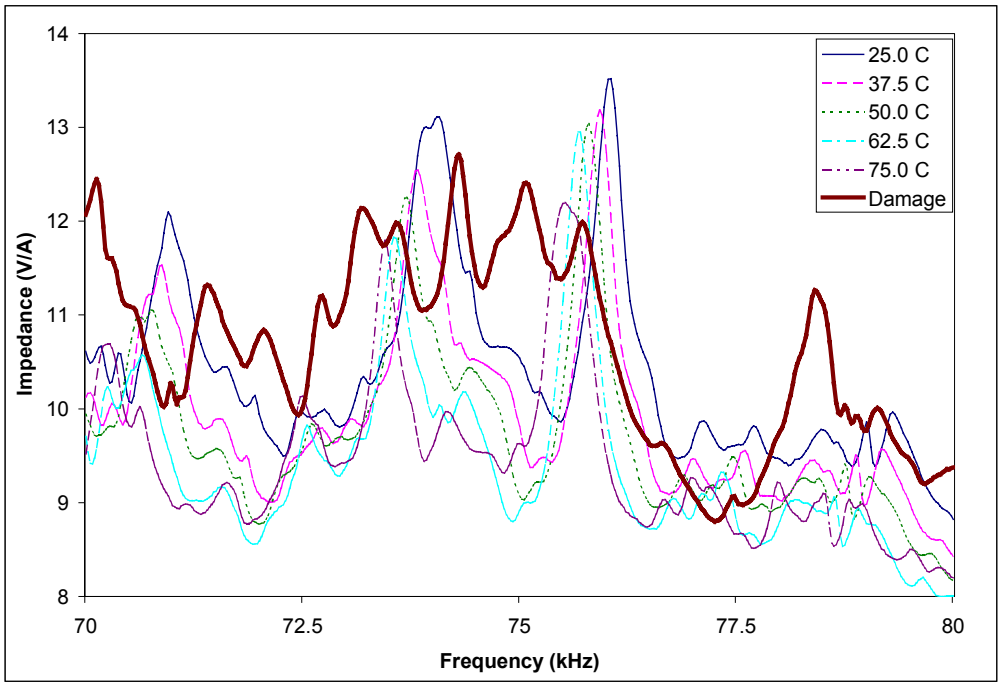

(a) Uncompensated impedance for temperature variations

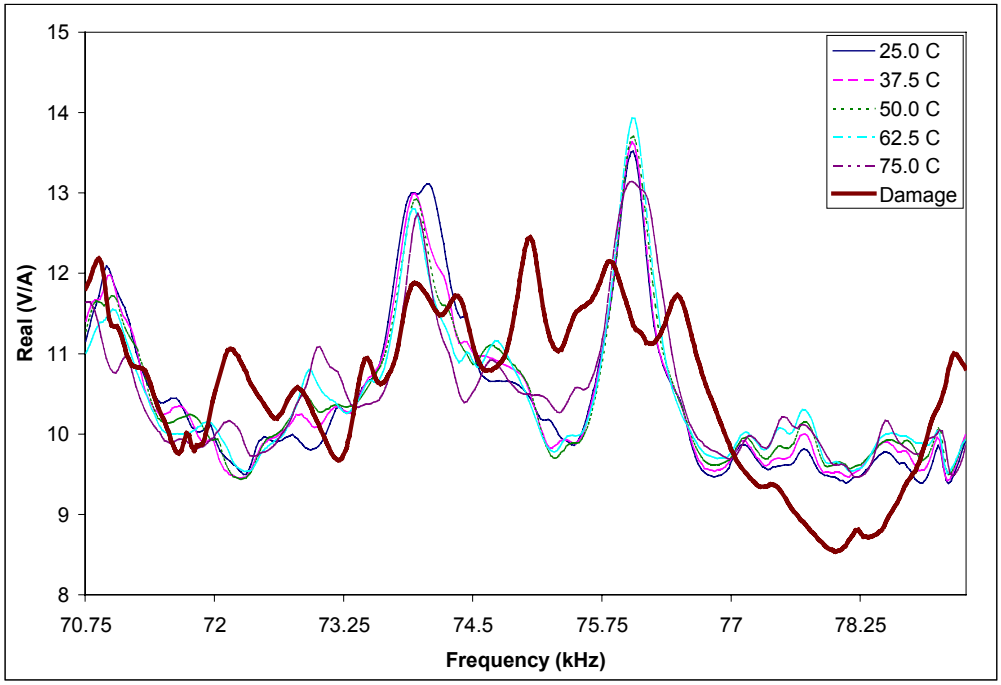

(b) Compensated impedance for temperature variations

Figure 2.9 Electrical impedance measurements with the temperature change in a bolted pipe joint

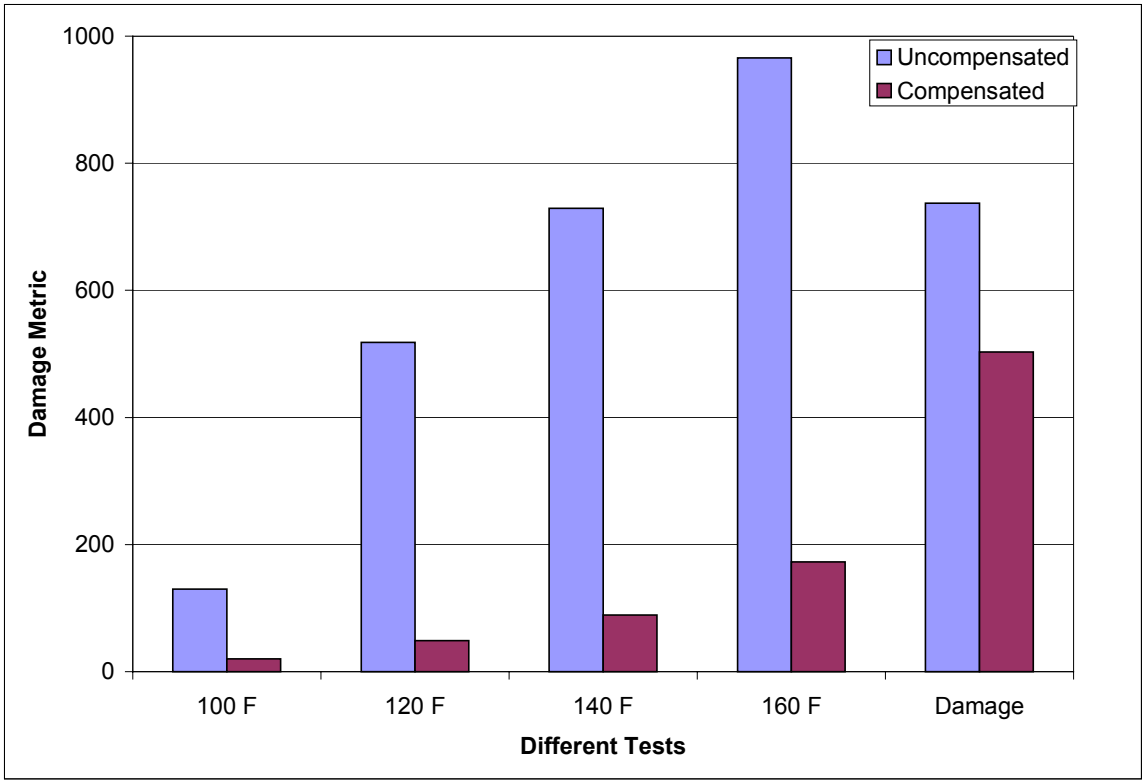

Figure 2.10 The damage metric chart of uncompensated and compensated impedance compared against the reference impedance measured at 25 $^{\circ}C$ - Bolted pipe joint

2.5.2 Abrasive wear of gears

Gears were chosen to test the impedance-based health monitoring under the temperature variation. This model is representative of a typical high precision part because of their high quality, and broad use. The detection of the most typical damage in gears, abrasive wear, was investigated. The AGMA 10 gears have a dimension of 63.5 mm. nominal diameter and 9.5 mm. Thickness, as shown in Figure 2.11. A PZT (Piezo Systems PSI-5A, 5 mm x 5 mm x 0.254 mm) was bonded for the acquisitions of impedance over the selected frequency range (190-220 kHz) at five temperature levels; 25, 37.5, 50, 62.5 and 75 $^{\circ}C$. After measuring the impedance at each level of temperature, The abrasive wear was created by filing one tooth across to the PZT sensor, at temperature 20 $^{\circ}C$. All of the impedance measurement were compensated and compared against the reference measurement, taken at temperature 25 $^{\circ}C$.

The results of compensated and uncompensated impedance measurements are shown in Fig. 2.12. Temperature effects on electrical impedance, shifting sharp peaks horizontally and changes in peak magnitude, were clearly observed. The fluctuations of magnitude are less pronounced compared to the previous experiment because there is no joint present in this setup, which act as a major source of changes in damping. It is very difficult to distinguish the damaged impedance measurement from temperature varying curves. However, by proposed temperature compensation procedure, the detection of abrasive wear was found to be successful, as shown in figures. After compensating all the measurements, the important deviation of the impedance curve (damaged one) around frequency range 194 kHz were clearly observed. Considering that damage is in incipient stage and wear usually occurs at several teeth at the same time, this method would be able to detect damage anywhere in the gear, even in the presence of relatively large temperature variations. Damage metric charts demonstrates the results more clearly, as can be seen in Fig. 2.13.

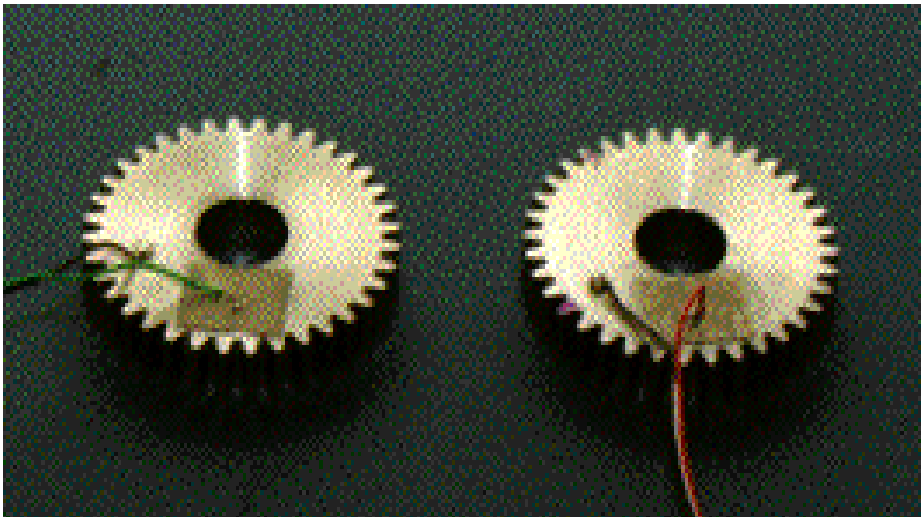

Figure 2.11 Detection of abrasive wear in gears was investigated.

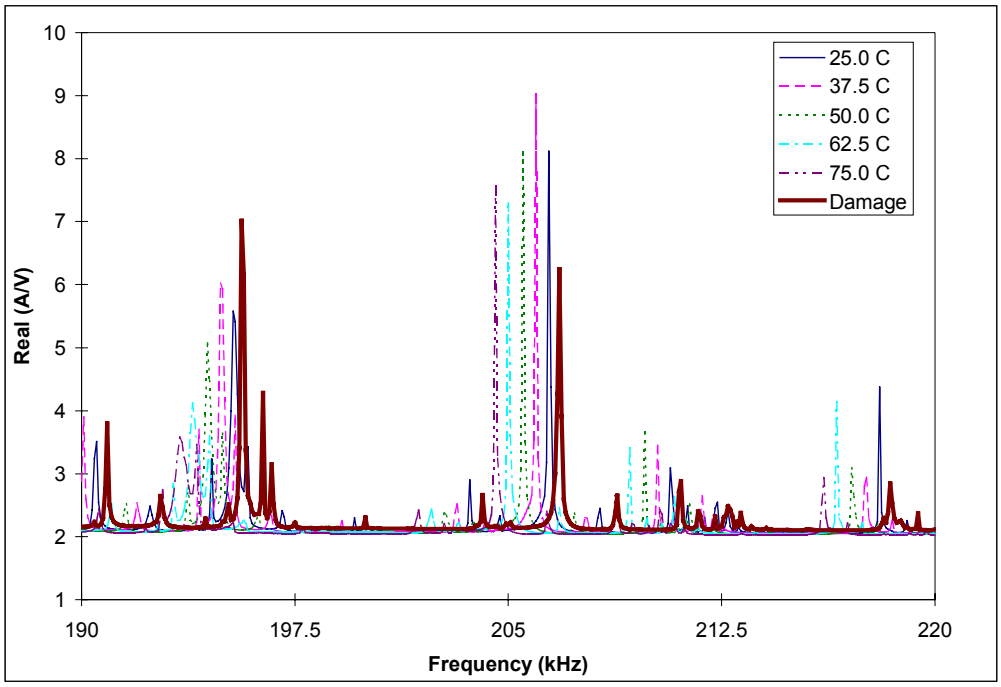

(a) Uncompensated Impedance

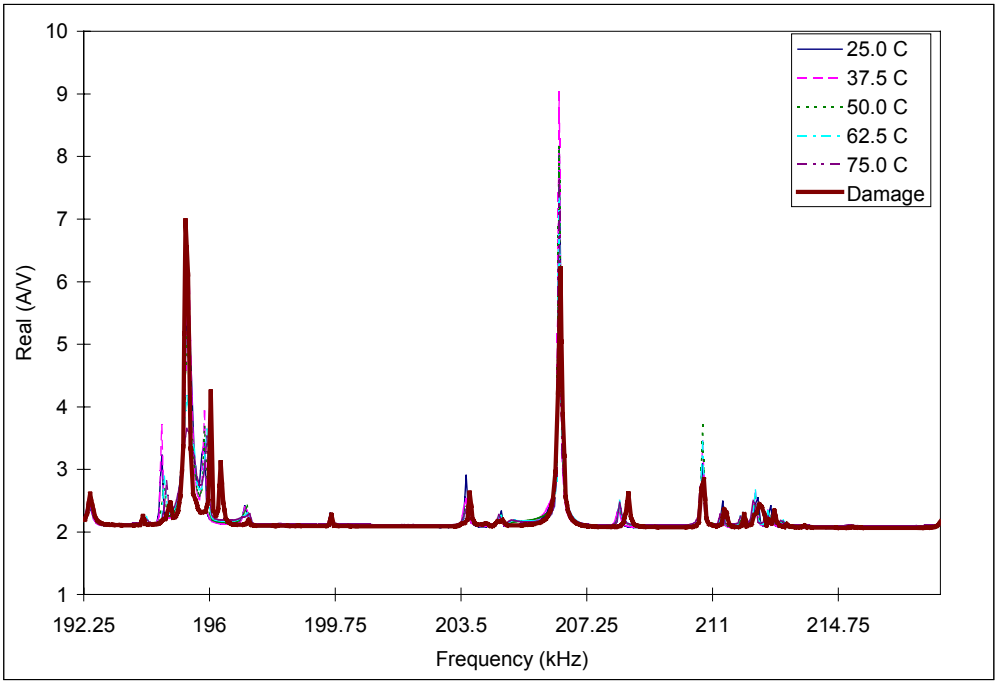

(b) Compensated Impedance

Figure 2.12 Electrical impedance with the temperature change in gear

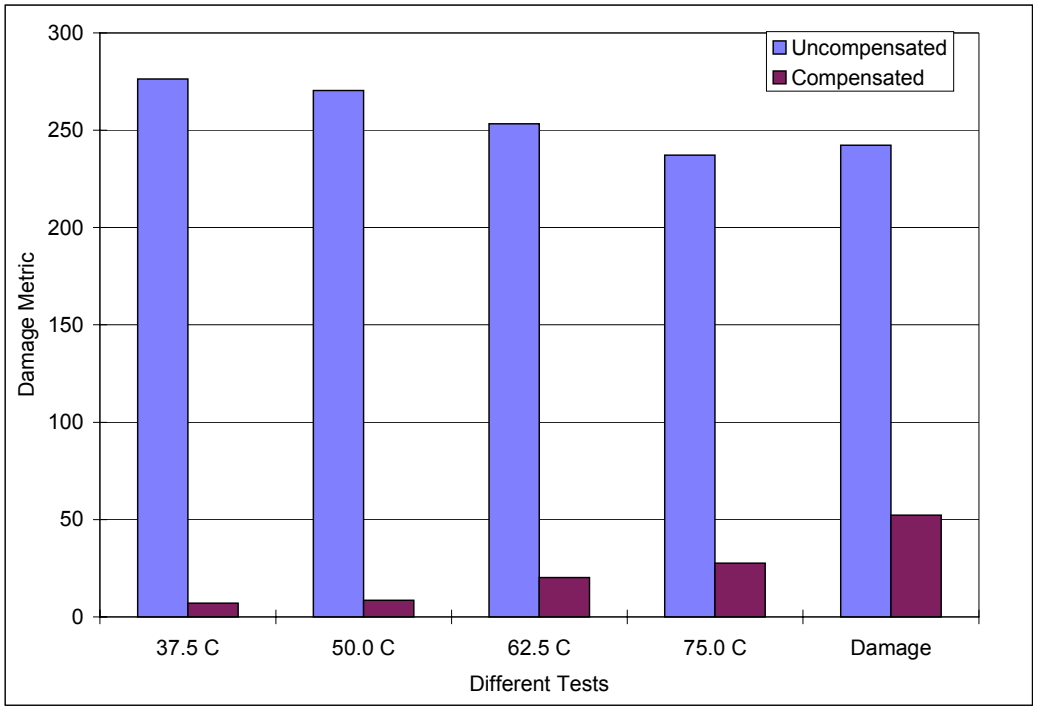

Figure 2.13 The damage metric chart of uncompensated and compensated impedance compared against the reference impedance measured at 25 $^{\circ}C$ - Gear

2.5.3 Delaminations of composite reinforced Patches

From a previous experiment (Chaudhry *et al.*, 1995), it has been shown that composite reinforced structures have relatively small sensing regions, compared with the steel structures. In addition, with different thermal expansion coefficients and Young's modulus changes with respect to temperature, it was expected that temperature variation would be more irregular in composite reinforced structures.

The detection of delaminations of aluminum plate and a bonded composite patch was investigated under the same temperature ranges used previous experiments (Figure 2.14). The bond between the base metallic panel and the reinforcing high-strength composite patch is critical to ensure the integrity of the composite structure. The de-bond is created by inserting a flattened screw-driver between the composite patch and the base plate in depth of 10 mm.

As expected, this application showed the most significant temperature variation. It was observed that, with the increasing the temperature, the dynamic interaction between PZT and structure is decreasing, almost flattening the sharp peaks in the electrical impedance versus frequency plot at the temperature level of 75 $^{\circ}C$. The temperature compensation technique could not be applied for this large variation. Up to 62.5 $^{\circ}C$, however, the compensation procedure is carried out successfully and clearly distinguish the presence of damage. Only the results of 25 - 62.5 $^{\circ}C$ temperature range are shown in Fig 2.15 and 2.16.

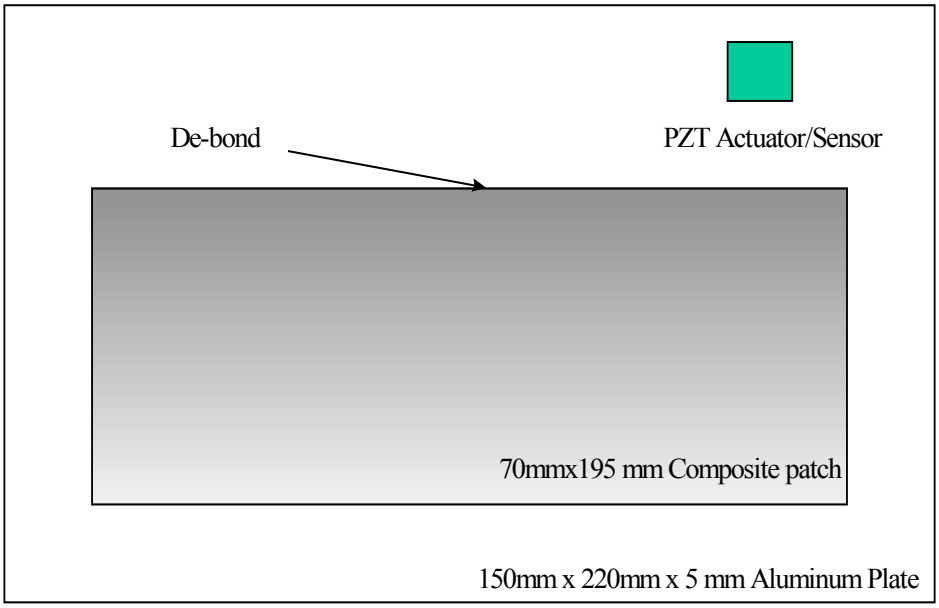

Figure 2. 14 Experimental setup for composite reinforced aluminum plate

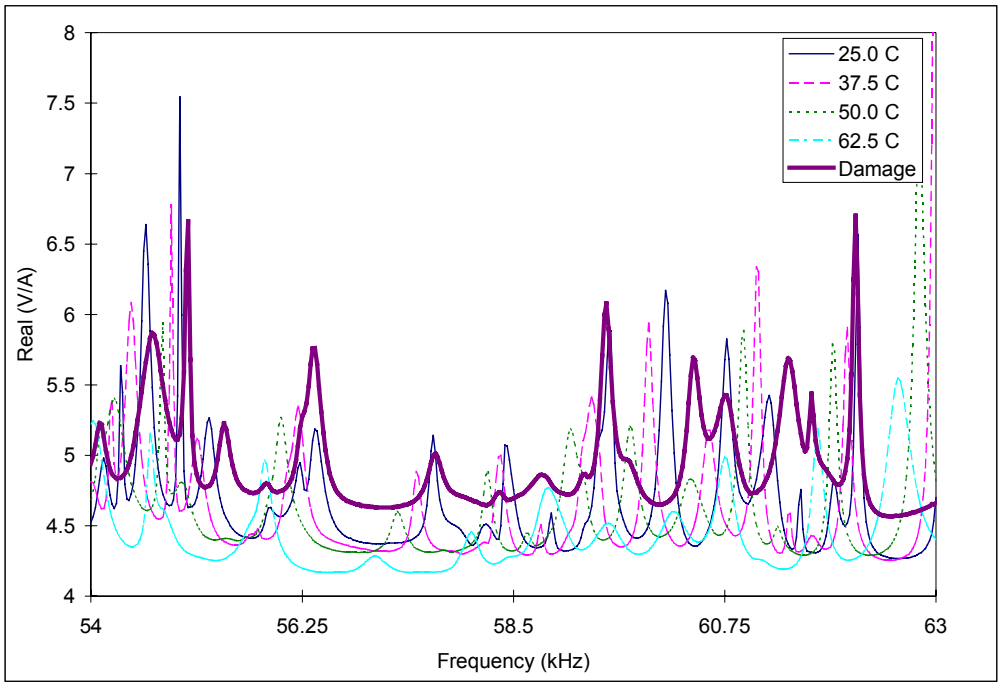

(a) Uncompensated Impedance

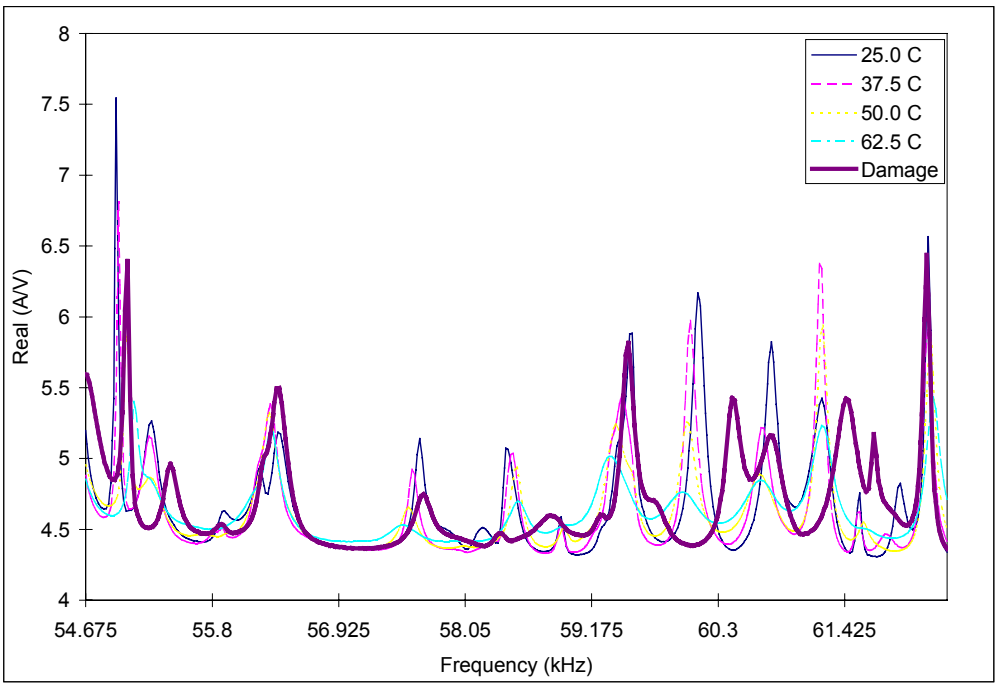

(b) Compensated Impedance

(c)

Figure 2.15. Electrical impedance with the temperature change in composite reinforced aluminum plate.

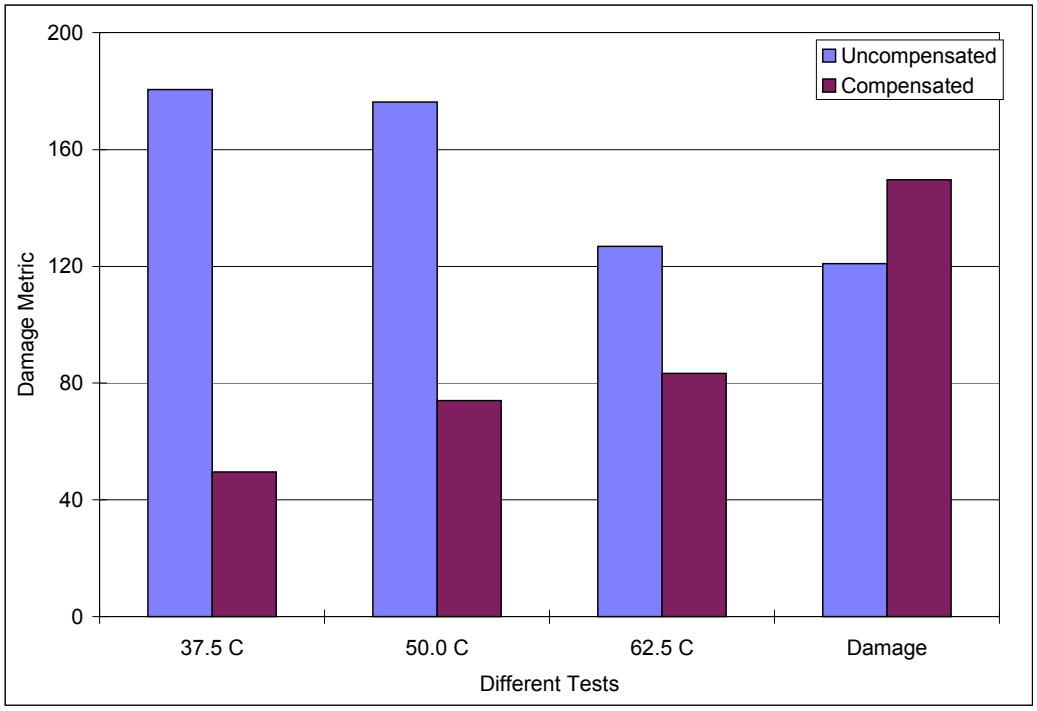

Figure 2.16. The damage metric chart of uncompensated and compensated impedance compared against the reference impedance measured at 25 $^{\circ}C$ - composite reinforced aluminum plate

2.6 Summary

Contrary to most structural health monitoring techniques, which are tested under a controlled temperature condition, or require exact temperature information when the measurements are taken, the impedance-based health monitoring technique was investigated under significant varying temperature condition. It has been found that the temperature change significantly influenced both the PZT sensor-actuators and the structure being monitored. Temperature changes cause vertical and horizontal shifts of the signature pattern in the impedance versus frequency plot, while damage causes somewhat irregular changes.

Based on this observation, an empirical temperature compensation technique was developed to remove the temperature effects from the impedance-based structural health monitoring

method. The advantages of the empirical approach include: i) it can be applied to complex structures since it does not require any model; and ii) it does not need temperature measurements. The compensation technique is a software correction based on vertical and horizontal translation of the signature pattern in the impedance plot. The experiments on a bolted pipe joint, a gear, and a composite reinforced aluminum plate have shown that the empirical temperature compensation technique could minimize the temperature effects. By this compensation procedure, it has been demonstrated that the impedance-based structural health monitoring technique is able to detect incipient-type damage such as loosening a bolt by 1/6 turn, abrasive wear in gears, and delaminations of composite reinforced patches, even with significant temperature variations.

In conclusion, the impedance-based structural health monitoring technique has enhanced the capability to detect incipient type damage in complex structures under the presence of significant temperature variation with the aid of the compensation procedure.